# Manual Measurement of Retinal Bifurcation Features

Bashir Al-Diri, Andrew Hunter, David Steel and Maged Habib

***Abstract*— This paper introduces a new computerized tool for accurate manual measurement of features of retinal bifurcation geometry, designed for use in investigating correlations between measurement features and clinical conditions. The tool uses user-placed rectangles to measure the vessel width, and lines placed along vessel center lines to measure the angles. An analysis is presented of measurements taken from 435 bifurcations. These are compared with theoretical predictions based on optimality principles presented in the literature. The new tool shows better agreement with the theoretical predictions than a simpler manual method published in the literature, but there remains a significant discrepancy between current theory and measured geometry.**

## I. INTRODUCTION

The retinal vascular network consists of branching arterial and venous trees that originate from the optic nerve head and progressively bifurcate into smaller branches that spread out across the retina. The vascular network is believed to be governed by physiological principles that optimize its efficiency [1]. Theory suggests that the branching diameters and angles at bifurcations should follow patterns that achieve a compromise between the requirements for minimum lumen volume, minimum pumping power and minimum drag force on endothelial cells [2], [3], [4], although there may be additional unmodelled principles at work (e.g. "watershed" constraints to service the full retinal surface). Vascular diseases may lead to damaging changes, and thus measurement of the geometry may be diagnostic or predictive of pathology. It is therefore of great interest to accurately measure the vascular geometry [5]. This paper introduces a computer-aided tool for manual measurement of retinal bifurcations which is able to yield accurate measurements.

The rest of the paper is structured as follows: Section II presents a background description of the geometric features of retinal bifurcations together with a theoretical analysis of the retinal vasculature. Section III describes the data set used. Section IV introduces the new method for measuring retinal bifurcation features; section V analyzes the performance of the method by comparing results with theory and a benchmark study from the literature, and section VI concludes the paper.

Bashir Al-Diri is with the Lincoln School of Computer Science, University of Lincoln, UK baldiri@lincoln.ac.uk

Andrew Hunter is the Dean of Research, University of Lincoln, UK

David Steel is with Sunderland Eye Infirmary, a Consultant Ophthalmologist, UK

Maged Habib is with Sunderland Eye Infirmary, a Specialist Registrar in Ophthalmology, UK

## II. PREVIOUS WORK

The basic measurements associated with a bifurcation, the branching angles ($\theta$, $\theta_1$ and $\theta_2$) and the diameters ($d_1$, $d_2$ and $d_3$) are shown in Figure 1. These are used to derive features that reflect the relationships between the various segment widths and the branching angles:

- The *bifurcation index*, $\lambda = \frac{d_2}{d_1}$, [6] is also called the degree of asymmetry; it is determined by dividing the diameter of the smaller child, $d_2$, by the diameter of the larger child, $d_1$; consequently, $0 < \lambda \leq 1$.
- The *asymmetry ratio*, $\alpha = \frac{d_2^2}{d_1^2}$, is the cross-sectional area of the smaller branch divided by that of the larger [2]; $0 < \alpha \leq 1$.
- The *diameter ratios*, $\lambda_1 = \frac{d_1}{d_0}$ and $\lambda_2 = \frac{d_2}{d_0}$, are the diameters of children divided by the diameter of the parent segment at a bifurcation [7].
- The *area ratio*, $\beta = \frac{d_1^2+d_2^2}{d_0^2}$, is the sum of the cross-sectional areas of the two branches divided by that of the parent segment at a bifurcation [2].
- The *junction exponent(k)*, $d_0^k = d_1^k + d_2^k$ characterizes the relationship between segment diameters.

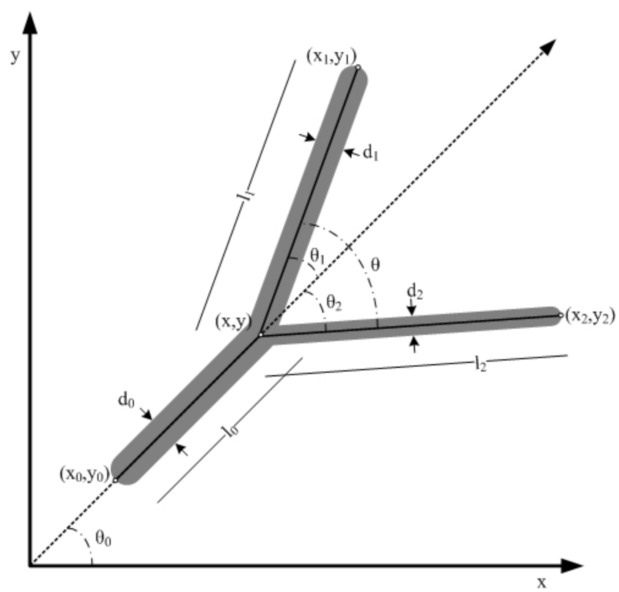


Fig. 1. The basic bifurcation features: diameters ($d_i$) and bifurcation angles ($\theta, \theta_i$).

The bifurcation index, $\lambda$, and the asymmetry ratio, $\alpha$, are measurements of the degree of asymmetry. Values of $\lambda$ and $\alpha$ near 1.0 indicate a rapid branching rate. The bifurcation is symmetrical if its $\lambda$ or $\alpha$ equal unity, which means that the widths of the branch segments are equivalent. If these factors are less that unity then the bifurcation is asymmetric or non symmetric; severe asymmetry holds when these factors approach a zero value. Theory suggests that, in a healthy retina, the branching angles and diameters should take values that optimize the efficiency of the entire vascular network. In particular, [8] suggests that the branching geometry should show good agreement with the *power law*, where the *junction exponent* $k$, given by $r_0^k = r_1^k + r_2^k$ (where $r_i = d_i/2$ is the radius of the vessel) should be equal to 3. In contrast, [9] proposed that if the branching angle is considered, the optimum rate of energy is obtained when $r_0^2 = r_1^2 \cos\theta_1 + r_2^2 \cos\theta_2$. The power laws can be re-expressed with respect to the asymmetry ratio to predict the area ratio:

$$\beta = \frac{d_1^2 + d_2^2}{d_0^2} = (1+\alpha)(1+\alpha^{k/2})^{-2/k}, \quad (1)$$

the diameter ratios:

$$\lambda_1 = \frac{d_1}{d_0} = (1+\alpha^{k/2})^{-1/k},\ \lambda_2 = \frac{d_2}{d_0} = \alpha^{1/2}(1+\alpha^{k/2})^{-1/k} \quad (2)$$

and the bifurcation angles for minimum pumping power and lumen volume:

$$\cos\theta_1 = \frac{\lambda_1^{-4} + 1 - \lambda^4}{2\lambda_1^{-2}}, \cos\theta_2 = \frac{\lambda_1^{-4} + \lambda^4 - 1}{2\lambda^2\lambda_1^{-2}}, \quad (3)$$

and for minimum drag and lumen surface:

$$\cos\theta_1 = \frac{\lambda_1^{-2} + 1 - \lambda^2}{2\lambda_1^{-1}}, \cos\theta_2 = \frac{\lambda_1^{-2} + \lambda^2 - 1}{2\lambda\lambda_1^{-1}}, \quad (4)$$

## III. MATERIALS

To test the new tool we selected 21 retinal images from the fundus image database of the diabetic retinopathy clinic at Sunderland Eye Infirmary. Retinal photography was performed on all patients according to a standardised protocol as part of their routine clinical care. Mydriasis was induced using tropicamide ($1\%$) eye drops. All images were independently graded by a qualified diabetic retinopathy grader adopting the modified classification developed for the EURODIAB Insulin-dependent diabetes mellitus complication study [10]. They were graded as follows: 12 images are normal, one has minimal non-proliferative retinopathy, three have moderate non-proliferative retinopathy, two have severe non-proliferative retinopathy and three have proliferative retinopathy. There are 435 marked junctions. Approximately $2\%$ of junctions are trifurcations [11]; we treat these as two consecutive bifurcations, where the first child segment of the first junction is the parent segment of the second junction.

## IV. Markup Tool for Bifurcation Geometry

We developed a new method to manually measure the retinal vessel widths using a computerized tool. This task is challenging as the vessels are typically blurred and curved. The vessel widths are measured by aligning rectangles over each segment; see Figure 2b. To place a rectangle the observer first nominates two points along the approximate segment centerline, and then a third on one of the segment edges. An aligned rectangle is drawn based on these points. The observer may then click to either side of the rectangle to adapt its width, and can click around its corners to adjust its direction. The observer keeps adapting the width and direction parameters until satisfied that the rectangle is correctly aligned. This method is effective as the width is judged along a short length of the vessel, which is easier than judging across a single profile (compare with [12], who calculates the width on five local cross sections with two pixel separation). The junction angles are nominated by first clicking to place an intersection point, and then clicking to place the ends of the three vessel centerlines; see figure 2a. The user may then click next to the intersection and end points as many times as desired to adjust the positions. The ability to refine the placement of rectangles and lines is crucial in allowing users to obtain a satisfactory result. The tool also presents the image junction zoomed up (using $8 \times 4$ blocks per pixel), but allows the user to place the measurement aids at full screen resolution, and thus to sub-pixel accuracy, which exploits the human ability to perceive at this level by exploiting anti-aliasing effects. The tool is implemented in MATLAB, and can be downloaded from http://ReviewDB.lincoln.ac.uk

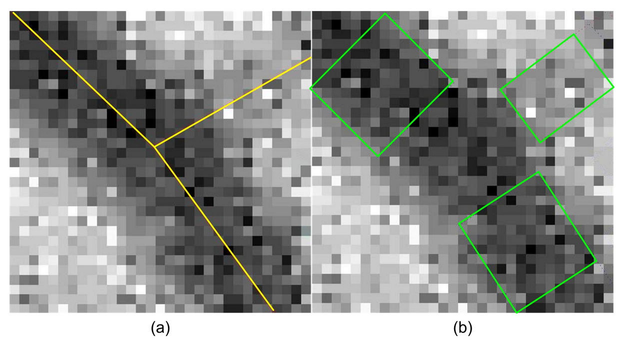


Fig. 2. (a) Defining bifurcation angles by drawing lines from the intersection point along segment centerlines. (b) Defining segment widths by placing three rectangles on the segment ends, choosing two points along the centreline and a point on the edge of the segment.

## V. RESULTS

Descriptive statistics of the 435 bifurcation measurements are given in table I.

| | Min | Max | Mean | Std E | Std D | Var |
|---|---|---|---|---|---|---|
| $d_0$ | 4.67 | 19.78 | 9.47 | 0.13 | 2.69 | 7.23 |
| $d_1$ | 3.78 | 17.51 | 8.37 | 0.12 | 2.48 | 6.16 |
| $d_2$ | 1.06 | 12.91 | 6.34 | 0.08 | 1.72 | 2.97 |
| $\theta$ | 43.75 | 132.32 | 80.17 | 0.70 | 14.62 | 213.87 |
| $\theta_1$ | -18.09 | 81.26 | 24.82 | 0.76 | 15.82 | 250.14 |
| $\theta_2$ | 10.17 | 97.72 | 55.34 | 0.82 | 17.16 | 294.52 |

TABLE I

Descriptive statistics of retinal junction features: the parent width ($d_0$), first child segment width ($d_1$), second child segment width ($d_2$), bifurcation angle ($\theta$) and branch angles ($\theta_1$, $\theta_2$).

|  | Min | Max | Mean | Std E | Std D | Var |
|---|---|---|---|---|---|---|
| $\alpha$ | 0.01 | 1.00 | 0.63 | 0.01 | 0.22 | 0.05 |
| $\lambda$ | 0.11 | 1.00 | 0.78 | 0.01 | 0.15 | 0.02 |
| $\lambda_1$ | 0.61 | 1.05 | 0.88 | 0.00 | 0.07 | 0.01 |
| $\lambda_2$ | 0.11 | 0.95 | 0.69 | 0.01 | 0.13 | 0.02 |

TABLE II

DESCRIPTIVE STATISTICS OF RETINAL BIFURCATION GEOMETRICAL FEATURES: THE ASYMMETRIC RATIO ($\alpha$), BIFURCATION INDEX ($\lambda$), FIRST DIAMETER RATIO ($\lambda_1$) AND SECOND DIAMETER RATIO ($\lambda_2$).

When a parent segment branches, the larger diameter branch should have a smaller deflection angle from the parent segment direction than the smaller diameter branch [13]. Theory suggests some limitations on branching angles – $0 \leq \theta_1 < 90°$, $0 \leq \theta_2 \leq 90°$, $\theta_1 \leq \theta_2$. In fact, $\theta_1 < 0$ in about 3% of cases (when the vessel branches inside a bend; see figure 3), which consequently leads to $\theta_1 > \theta$, and in 14% of cases $\theta_1 > \theta_2$. However, the rule that $\theta_2 > 0$ holds consistently. The results of [3] suggest that the vascular junction is optimal when $75° < \theta < 102°$; in our study, only 56% fall into this optimal range; in 37% $\theta < 75°$ and in 7% $\theta > 102°$. Theoretically, we expect $d_0 \geq d_1 \geq d_2$. In 1% of

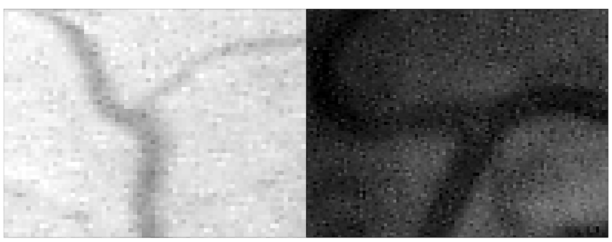

(a) (b)

Fig. 3. Very large branching angles situated on curving vessels.

cases we examined $d_0 < d_1$ , apparently due to a narrowing of the parent (see figure 4); however, $d_0 > d_2$ consistently.

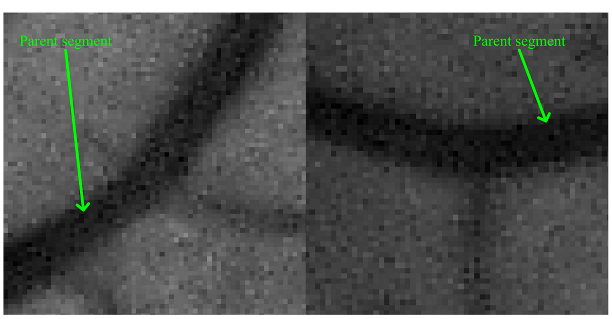


(a) (b)

Fig. 4. Bifurcations where the parent segment diameter is smaller than the first child segment diameter.

We also discovered that in 14% of cases $\theta_1 > \theta_2$, where we accepted the definition that the first child is that with the larger diameter, $d_1 > d_2$. However, bearing in mind that vessel widths may vary along the length, an alternative and more robust definition is formed by noting that each child connects to a vascular sub-network, and that the first child is the one with the bigger sub-network. Using this definition we find that in 5% of cases $d_2 > d_1$ and 9% of cases $\theta_1 > \theta_2$. These findings may be due to measurement errors, natural variations, effects of vessel curvature or pathological changes. Consequently, the features $\alpha$, $\lambda$ and $\lambda_1$, which theoretically should be less than one, sometimes exceed it. These features depend on the order of the first and second segments. The descriptive statistics for these features are given in table II.

Despite its popularity and strong theoretical basis, the junction exponent $k$ is an over-sensitive parameter. Although physiological principles suggest an optimal value of 3, values between 1.0 and 5.0 have been reported in [14], [15], [16], [17], [18]. In our study the estimated value of $k$ varies even more widely, with mean 3.96 and standard deviation 2.71, and in some cases (where $d_0 < d_1$) is undefined. The area ratio parameter, $\beta$, which also defines a relationship between the radius of the three segments, is more stable and hence useful. The literature [3] indicates that the junction is highly optimal when the area ratio $\beta$ is between 1.15 and 1.4 (for a symmetrical bifurcation, $\beta = 1.26$). In our study, the mean is 1.27, the standard deviation is 0.22, and the range is [0.66 1.86]. The optimality parameter ($\rho$) [19] which measures deviation of junction exponents from the optimal value of 3, is calculated as:

$$\rho = [d_0^3 - (d_1^3 + d_2^3)]^{(1/3)}/d_0 \tag{5}$$

In our study, the mean is $-0.12$, the standard deviation is 0.56, and the range is [$-0.92$ 0.85]. Some theoretical studies proposed that if the angle of branching is considered, the optimum rate of energy [9] is obtained when

$$r_0^2 = r_1^2 \cos\theta_1 + r_2^2 \cos\theta_2. \tag{6}$$

The Descriptive statistics for these features are given in table III.

|  | Min | Max | Mean | Std E | Std D | Var |
|---|---|---|---|---|---|---|
| $\beta$ | 0.66 | 1.86 | 1.27 | 0.01 | 0.22 | 0.05 |
| $k$ | 0.00 | 20.57 | 3.94 | 0.12 | 2.57 | 6.60 |
| $\rho$ | -0.92 | 0.85 | -0.12 | 0.03 | 0.56 | 0.32 |

TABLE III

DESCRIPTIVE STATISTICS OF RETINAL BIFURCATION GEOMETRICAL FEATURES: THE AREA RATIO ($\beta$), JUNCTION EXPONENT ($k$) AND OPTIMALITY PARAMETER ($\rho$).

## A. Theoretical Predictions

In this section we validate the tool by comparing the measured junction features with predictions from theory, following the methodology introduced in [5]. We also benchmark against the results reported in [5]. The theoretical predictions and measurements are presented in terms of $\beta$, $\lambda_1$, $\lambda_2$, $\theta_1$, $\theta_2$ and $\theta$ against $\alpha$ in figures 5 and 6. Each graph plots a pair of features against one another. The scatter points indicate the measurements; the lines represent the theoretical predicted curves: the solid line minimum lumen surface and drag, the dashed line minimum lumen volume and pumping power (see equations 3 and 4). To achieve a compromise between these conflicting requirements, theory suggests that the points should lie between these two lines.

The measured bifurcation features are characterized by a high degree of variability. This may be due to a combination of normal biological scatter [5] [20], the value of the power law exponent $k$ [4], experimental measurement errors, or intrinsic vascular variability [21]. Some of the variation may relate to pathology in those subjects with diabetic retinopathy. Table IV shows the percentage of the experimental data points within $10\%$ deviation around the theoretical curves. As a benchmark the corresponding statistics from Zamir [5] are shown, although we note that this uses a different different data set; there is thus an unknown degree of intra-experimental variation in the results. Zamir extracted measurements by projecting the retinal image at $\times 100$ magnification, manually tracing the vessel edges onto white paper, taking width measurements with vernier calipers, and drawing centre lines and using a protractor to measure angles.

| Features | Zamir | Al-Diri |
|---|---|---|
| $\beta$ | - | $42\%$ |
| $\lambda_1$ | $64\%$ | $75\%$ |
| $\lambda_2$ | $64\%$ | $76\%$ |
| $\theta$ | $60\%$ | $79\%$ |
| $\theta_1$ | $32\%$ | $42\%$ |
| $\theta_2$ | $48\%$ | $50\%$ |

TABLE IV

PERCENTAGE OF DATA POINTS LYING WITHIN A STRIP OF $10\%$ DEVIATION AROUND THE THEORETICAL CURVES. THE BENCHMARK FIGURES ARE TAKEN DIRECTLY FROM ZAMIR CITEVAS3.

Zamir reported that $55\%$ of $\beta$ data points lie within $20\%$ deviation from the theoretical predictions; the corresponding figure for the proposed technique is $76\%$. It is clear that a greater proportion of the measurements taken using our tool accord with theoretical predictions than were reported by Zamir, and we speculate that this is due to greater accuracy in the measurements. However, in the absence of a reference standard it is not possible to verify this supposition.

## VI. CONCLUSIONS

This paper introduces a tool for the accurate measurement of retinal vascular junction geometry, and discusses the features that may be extracted from these measurements. The tool is intended to support research into the underlying principles governing retinal bifurcation geometry, and to investigate the effect of pathologies on it. The relationship of the actual measurements taken on a sample data set to theoretical predictions based on some previously published optimality principles are studied. There is a good degree of compliance with the theory, but with a significant amount of unexplained variability. In future work we will investigate whether a more sophisticated theoretical model is able to provide better correlation between theory and experimental

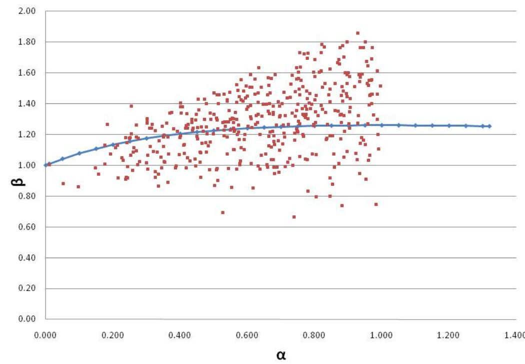


a: $\beta$ vs. $\alpha$.

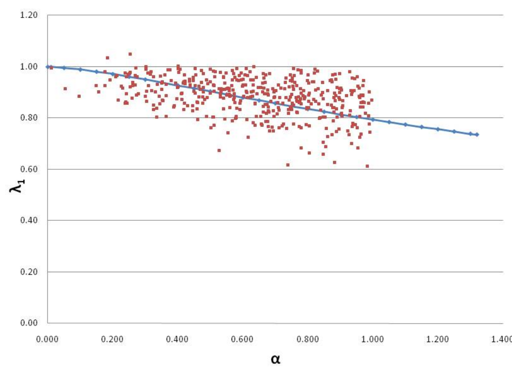


b: $\lambda_1$ vs. $\alpha$.

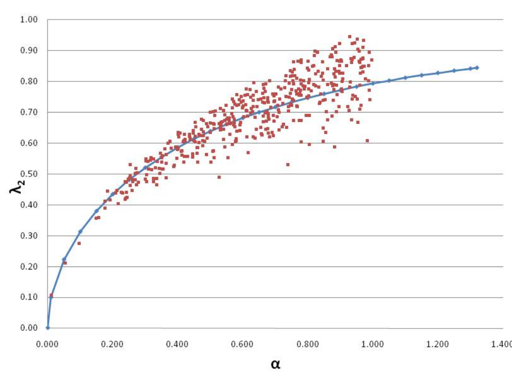


c: $\lambda_2$ vs. $\alpha$.

Fig. 5. Relationship between features derived from vessel widths. The theoretical curves assume $k = 3$; data points show the manual measurements on the test data set.

measurements, analyze the performance of the tool for inter- and intra-observer repeatability, and investigate the relationship of various diseases to bifurcation geometry.

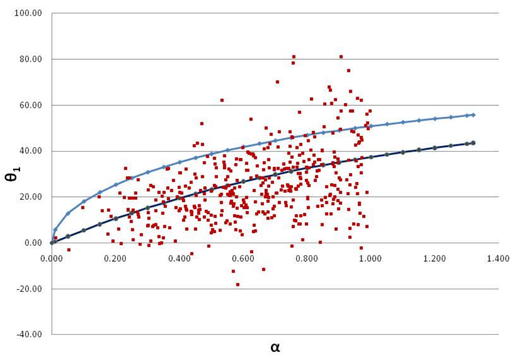


a: $\theta_1$ vs $\alpha$.

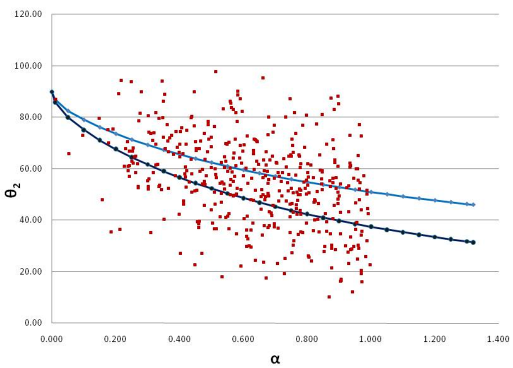


b: $\theta_2$ vs $\alpha$.

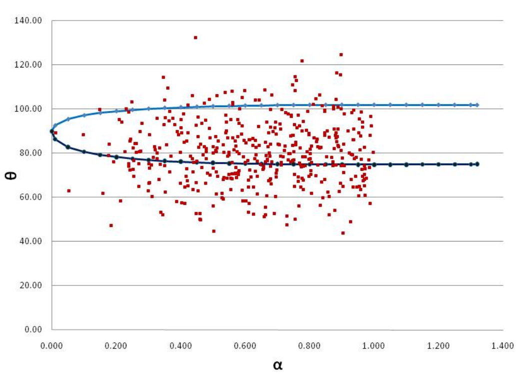


c: $\theta$ vs $\alpha$.

Fig. 6. Relationship between angles. The theoretical curves assume $k = 3$; data points show the manual measurements.

## References


[1] M. Zamir and N. Brown, "Arterial branching in various parts of the cardiovascular system," *American Journal Of Anatomy*, vol. 163, no. 4, pp. 295–307, April 1982.

[2] M. Zamir, "Nonsymmetrical bifurcations in arterial branching," *The Journal Of General Physiology*, vol. 72, pp. 837–845, December 1978.

[3] ——, "Optimality principles in arterial branching," *Journal Of Theoretical Biology*, vol. 62, pp. 227–251, 1976.

[4] M. Zamir and J. A. Medeiros, "Arterial branching in man and monkey," *The Journal Of General Physiology*, vol. 79, pp. 353–360, 1982.

[5] M. Zamir, J. A. Medeiros, and T. K. Cunningham, "Arterial bifurcations in the human retina," *The Journal Of General Physiology*, vol. 74, pp. 537–548, 1979.

[6] M. Zamir, "Distributing and delivering vessels of the human heart," *The Journal Of General Physiology*, vol. 91, pp. 725–735, 1988.

[7] R. Karch, F. Neumann, M. Neumann, and W. Schreiner, "Staged growth of optimized arterial model trees," *Annals of Biomedical Engineering*, vol. 28, no. 5, pp. 495–511, May 2000.

[8] M. Zamir, P. Sinclair, and T. H. Wannacott, "Relation between diameter and flow in major branches of the arch of the aorta," *Journal Biomechanics*, vol. 25, no. 11, pp. 1303–1310, 1992.

[9] J. K.-J. Li, *Dynamics Of The Vascular System*, ser. Bioengineering and Biomedical Engineering. World Scientific, 2004.

[10] S. Aldington, E. Kohner, S. Meuer, R. Klein, A. Sjolie, and T. E. I. C. S. Group, "Methodology for retinal photography and assessment of diabetic retinopathy: the eurodiab iddm complications study," *Diabetologia*, vol. 38, no. 4, pp. 437–444, April 1995.

[11] Y. Zhou, G. S. Kassab, and S. Molloi, "On the design of the coronary arterial tree: A generalization of murrays law," *Physics in Medicine and Biology*, vol. 44, no. 12, pp. 2929–2945, December 1999.

[12] N. Chapman, N. Witt, X. Gao, A. A. Bharath, A. V. Stanton, S. A. Thom, and A. D. Hughes, "Computer algorithms for the automated measurement of retinal arteriolar diameters," *British Journal of Ophthalmology*, vol. 85, pp. 74–79, 2001.

[13] M. Zamir, "The role of shear forces in arterial branching," *The Journal Of General Physiology*, vol. 67, no. 2, pp. 213–222, 1976.

[14] A. Kamiya and T. Togawa, "Optimal branching structure of the vascular tree," *Bulletin of Mathematical Biophysics*, vol. 34, no. 4, pp. 431–438, 1972.

[15] S. Rodbard, "Vascular caliber," *Cardiology*, vol. 60, pp. 4–49, 1975.

[16] M. Zamir, "Shear forces and blood vessel radii in the cardiovascular system," *The Journal Of General Physiology*, vol. 69, pp. 449–461, 1977.

[17] T. F. Sherman, "On connecting large vessels to small: The meaning of murray's law," *The Journal Of General Physiology*, vol. 78, pp. 431–453, October 1981.

[18] M. J. Woldenberg and K. Horsfield, "Finding the optimal length for three branches at a junction," *Journal Of Theoretical Biology*, vol. 104, no. 2, pp. 301–318, 1983.

[19] N. Chapman, G. Dell'omo, M. Sartini, N. Witt, A. Hughes, S. Thom, and R. Pedrinelli, "Peripheral vascular disease is associated with abnormal arteriolar diameter relationships at bifurcations in the human retina," *Clin Sci (Lond)*, vol. 103, no. 2, pp. 111–116, 2002.

[20] M. Zamir, "Arterial branching within the confines of fractal l-system formalism," *The Journal Of General Physiology*, vol. 118, pp. 267–275, 2001.

[21] ——, "Fractal dimensions and multifractility in vascular branching," *Journal Of Theoretical Biology*, vol. 212, pp. 183–190, 2001.